Dense-packing crystal structures of physical tetrahedra

Yoav Kallus and Veit Elser

Dense packing crystal structures of physical tetrahedra

Yoav Kallus and Veit Elser

Laboratory of Atomic and Solid-State Physics, Cornell University, Ithaca, New York, 14853

We present a method for discovering dense packings of general convex hard particles and apply it to study the dense packing behavior of a one-parameter family of particles with tetrahedral symmetry representing a deformation of the ideal mathematical tetrahedron into a less ideal, physical, tetrahedron and all the way to the sphere. Thus, we also connect the two well studied problems of sphere packing and tetrahedron packing on a single axis. Our numerical results uncover a rich optimal-packing behavior, compared to that of other continuous families of particles previously studied. We present four structures as candidates for the optimal packing at different values of asphericity, providing an atlas of crystal structures which might be observed in systems of nano-particles with tetrahedral symmetry.

Impenetrable (hard) mathematical bodies (e.g. spheres, spheroids, superballs, and polyhedra) have received much attention as models for the equilibrium behavior of systems of nano-particles and for the wealth of equilibrium and non-equilibrium structures they exhibit [1–6]. For the tetrahedron alone, quasicrystal structures, novel crystal structures, and glassy structures have been reported in numerical simulations [5–9]. However, in all cases, the tetrahedral particles studied were mathematically ideal (polyhedral) tetrahedra. By contrast, in an experiment which found that regular tetrahedra have random packings that are denser than observed for any other body, the tetrahedral macro-particles (dice) used had rounded edges and vertices [10, 11]. Tetrahedral nano-particles used as colloids are not only imperfectly-shaped tetrahedra, but are also sometimes soft, in the sense that the interactions beyond hard-core repulsion are significant [12–15]. In this paper, we attempt to characterize the packing behavior of physical, rather than mathematical, tetrahedra by studying a one-parameter family of particles with tetrahedral symmetry that interpolates between the mathematical tetrahedron on one end of the parameter's range and the sphere on the other end. We explore the effect of this parameter by constructing, using a *de novo* numerical search, candidate structures for the optimal packing of the different particles in the family.

A particle interpolating between the sphere and the regular tetrahedron can be achieved by a variety of constructions. The simplest construction, probably, is to place the centers of four unit spheres at the vertices of a regular tetrahedron with edges of length a and consider the volume at the intersection of all four spheres. We call the resulting figure a *tetrahedral puff* (Figure 1). For a special value of a, the tetrahedral puff is the Reuleaux tetrahedron (a three-dimensional version of the Reuleaux triangle, but not a solid of constant width) [16]. A more convenient parameter than this edge length is the asphericity γ, which is the ratio between the radii of the particle's circumscribing and inscribed spheres. The value $\gamma = 1$ obtained when the four spheres coincide corresponds to a sphere. The value $\gamma = 3$, which
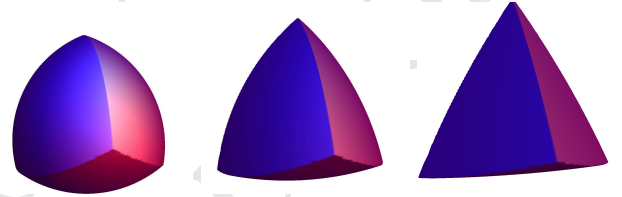

FIG. 1: (Color online) tetrahedral puffs of varying asphericity. From left to right, the asphericities of the puffs shown are $\gamma = 4/3, 2, 8/3$.

is the largest asphericity possible for a convex particle with tetrahedral symmetry and corresponds to a regular tetrahedron, is obtained in the limit that the four spheres intersect at a point. The Reuleaux tetrahedron is the puff with asphericity $\gamma = (3 + \sqrt{24})/5 \approx 1.58$.

To efficiently search for candidate optimal packing structures we run a numerical search for packings at increasing densities. To prevent overlaps between different particles in the structure we employ an overlap resolution step. In a packing of congruent particles, every particle can be obtained from a single primitive particle K by a rotation and a translation: $K_1 = R_1 K + r_1 = \{R_1 x + r_1 | x \in K\}$, where R_1, a rotation matrix, and r_1, a translation vector, parameterize the configuration of the particle K_1. We call an *exclusion projection* the operation of, for any two particles K_1 and K_2 that overlap, identifying the new set of configuration parameters (R_1', R_2', r_1', r_2') that resolves the overlap while minimizing the distance in configuration-space from the original configuration, (R_1, R_2, r_1, r_2). This is the projection in configuration-space to the set of non-overlapping configurations. Below we give the method of implementing this projection.

At high densities, however, we may have to resolve overlaps of a particle with multiple other particles, and the projection that applies to pairs cannot be used directly. Therefore, we introduce multiple independent copies (replicas) of the configuration parameters of each particle, so that after an exclusion projection, any pair of

particles will have at least one overlap-free pair of replicas. Another projection ensures that in the final structure obtained from the search all replicas of a single particle agree on its configuration. The two projections are not applied alternately, but instead composed with linear combinations to give the difference map iteration [17]. This scheme, called *divide and concur* ($D-C$), has previously allowed us to study dense packings of a variety of polyhedral and high-dimensional spherical particles, and is here generalized to any convex particle. Apart from the exclusion projection, described here, the rest of the application of the scheme to dense periodic packing discovery is described in Ref. [18].

Given a pair of particles (or replicas) in a configuration $(R_1, R_2, \mathbf{r}_1, \mathbf{r}_2)$ which overlaps, the exclusion projection resolves the overlap by identifying a new set of configuration parameters $(R'_1, R'_2, \mathbf{r}'_1, \mathbf{r}'_2)$ while minimizing the distance to the original configuration as defined by

$$d^2 = \sum_{i=1,2} ||\mathbf{r}_i - \mathbf{r}'_i||^2 + ||R_i - R'_i||^2, \qquad (1)$$

where the matrix norm is the Frobenius norm. The projection algorithm for a general convex particle is most easily expressed in terms of the particle's support function $h(\mathbf{u}) = \max_{\mathbf{x} \in K} \mathbf{u} \cdot \mathbf{x}$. If the support function $h(\mathbf{u})$ of K is known, then the support function of K_i is $h_i(\mathbf{u}) = \max_{\mathbf{x} \in K} \mathbf{u} \cdot R_i \mathbf{x} + \mathbf{u} \cdot \mathbf{r}_i = h(R_i^T \mathbf{u}) + \mathbf{u} \cdot \mathbf{r}_i$ [19].

By the separating plane theorem, K_1 and K_2 do not overlap if and only if a vector $\mathbf{u}$ exists such that $\Delta h(\mathbf{u}) = h_1(\mathbf{u}) + h_2(-\mathbf{u}) \le 0$ [19]. We can determine if such a vector exists by numerically minimizing $\Delta h(\mathbf{u})/||\mathbf{u}||$, which is bounded and attains a minimum over $\mathbf{u}$. If the minimum value of $\Delta h(\mathbf{u})/||\mathbf{u}||$ is positive, we must make the minimal change possible to the configuration parameters so that

$$h'_1(\mathbf{u}) + h'_2(-\mathbf{u}) = 0 \text{ for some } \mathbf{u}. \qquad (2)$$

If we relax the condition that R'_i is a rotation matrix, then we can reduce this constrained optimization problem to a simple unconstrained optimization problem in three vector variables. Namely, these vectors are $\mathbf{u}$, $\mathbf{v}_1 = R_1'^T \mathbf{u}$, and $\mathbf{v}_2 = R_2'^T \mathbf{u}$. Given these three vectors, the new configuration parameters which minimize (1) and satisfy (2) are given by

$$\mathbf{r}'_1 = \mathbf{r}_1 - \frac{\mathbf{u}}{2||\mathbf{u}||^2}\Delta h \qquad (3a)$$

$$\mathbf{r}'_2 = \mathbf{r}_2 + \frac{\mathbf{u}}{2||\mathbf{u}||^2}\Delta h \qquad (3b)$$

$$R'_i = R_i + \frac{\mathbf{u}}{||\mathbf{u}||^2}(\mathbf{v}_i^T - \mathbf{u}^T R_i), \qquad (3c)$$

where $\Delta h = h(\mathbf{v}_1) + h(-\mathbf{v}_2) + (\mathbf{r}_1 - \mathbf{r}_2) \cdot \mathbf{u}$ and the configuration distance is given by

$$d^2 = \frac{\Delta h^2/2 + ||\mathbf{u}R_1 - \mathbf{v}_1||^2 + ||\mathbf{u}R_2 - \mathbf{v}_2||^2}{||\mathbf{u}||^2}. \qquad (4)$$

And so, we have reduced the problem, as promised, to an unconstrained minimization of (4) over three vector variables. Note that (4) is invariant under uniform positive rescaling of $\mathbf{u}$, $\mathbf{v}_1$, and $\mathbf{v}_2$, and the resulting vanishing gradient direction must be taken into account when performing the minimization.

The restriction on R_i to be a rotation matrix, i.e. the requirement on the rigidity of the particle, as in Ref. [18], is restored in the concurrence constraint of the $D-C$ scheme. The projection of a general matrix into the subset of orthogonal matrices is as simple as taking its singular value decomposition and setting all the singular values to unity [20].

As a method for exploring dense configurations of general hard particles, we believe our projection-based method to be more direct and efficient when compared to event-driven MD simulations and stochastic MC methods [2]. Partly, the $D-C$ scheme draws its power from temporarily allowing non-physical configurations, with overlaps, non-concurring replicas, and non-rigid particles, but then systematically acting to minimize these non-physicalities. In MC simulations, such temporary allowance has also been observed to be critical in efficiently exploring structures at high density [8].

For a selection of puffs of different asphericities, we use the $D-C$ scheme to perform repeated *de novo* searches for periodic packings with $p = 1, 2, 3, 4, 6$, and 8 puffs per unit cell. The densest packing found for each value of γ is reported here as a candidate for the optimal packing structure. Every packing density that is reported here as putatively optimal for a puff of some asphericity has been reproduced by the numerical search at least 3 times from random initial conditions and if the structure has two puffs in the primitive unit cell, it has been reproduced in searches with both $p = 2$ and $p = 4$.

As suggested by the results of our numerical searches, four different packing structures are optimal at different asphericities, separated by one continuous structural transition and two abrupt ones. Of most interest are the structures of the optimal packing for puffs of small asphericity and large asphericity in the parameter ranges near the sphere and the tetrahedron respectively. The optimal packing structure for small asphericity, which we call the $\mathcal{S}_0$-structure (for *simple double lattice*), is a tetragonal double lattice – that is, the union of two lattices (with one particle per unit cell) that are related to each other by an inversion about a point (Figure 2) [21]. In the $\mathcal{S}_0$-structure, the puffs are arranged into square layers so that from each layer, the puffs stick out on one side in parallel ridges running in one direction and on the other side in parallel ridges running in a perpendicular direction. By stacking each consecutive layer with a 90° rotation, the ridges of one layer align with the ridges of the layer above it. In the limit $\gamma \to 1$, each layer approaches a square packing of spheres, and the $\mathcal{S}_0$-structure approaches the face-centered cubic sphere packing structure.

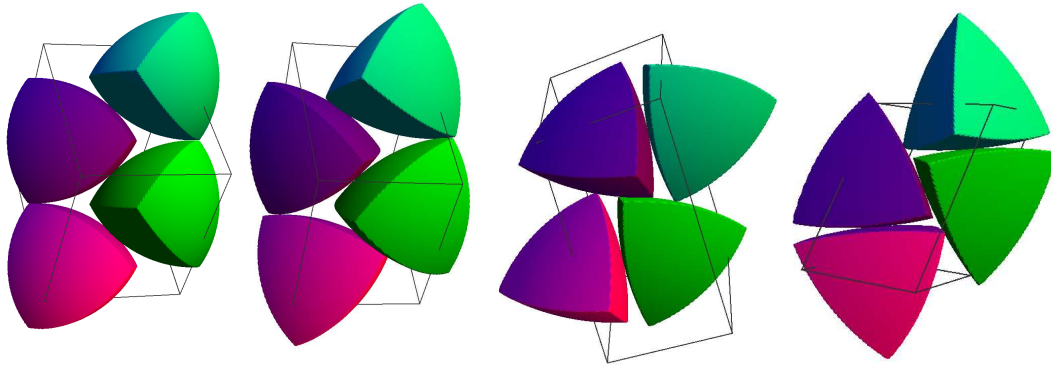For large asphericities, the optimal packing structure,

FIG. 2: (Color online) a unit cell of each of the four structures described, (from left to right) the $\mathcal{S}_0$-, $\mathcal{D}_1$-, $\mathcal{S}_1$-, and $\mathcal{D}_0$-structures. For the $\mathcal{S}_0$- and $\mathcal{S}_1$-structure, a unit cell consisting of two primitive unit cells is shown. In all cases, the purple (top-left) and pink (bottom-left) puffs are related by inversion to the green (bottom-right) and teal (top-right) puffs respectively. The $\mathcal{S}_0$-structure is a body-centered tetragonal crystal where the body-centered puff is inverted in orientation from the corner puffs. The $\mathcal{D}_1$-structure occurs when next-nearest square layers of the $\mathcal{S}_0$-structure come into contact, and its symmetry is broken by a re-orientation of different puffs of the same layer in different directions. By contrast, the $\mathcal{S}_1$-structure arises by an abrupt transition at both ends of the parameter interval on which it is optimal. In the $\mathcal{D}_0$-structure the mirror planes of the green and teal puffs, which form a dimer, are not aligned, so that both can be in contact with the purple puff. In the limit $\gamma \to 3$, the green and teal puffs become aligned and form a bipyramidal dimer. The structure becomes the dimer double lattice structure reported in Refs. [7, 9] as the densest known packing of regular tetrahedra.

which we call the $\mathcal{D}_0$-structure, is a *dimer double lattice* (i.e. each of the two inversion-related lattices is a lattice of dimers). The unit cell contains four puffs, two of which, which are in contact and form a shape similar to a triangular bipyramid, are related by inversion to the other two (Figure 2). We call each of the two inversion related pairs a dimer, in analogy with the dimer double lattice of Refs. [7, 9], which is the limit of the $\mathcal{D}_0$-structure as $\gamma \to 3$, and is the densest known packing of regular tetrahedra. In this limit, each dimer exactly forms a triangular bipyramid. Note that away from $\gamma = 3$, the mirror planes of the two puffs constituting the dimer are not aligned with each other, making the dimer look twisted. This allows both puffs to form a contact with a nearby puff (see Figure 2), which in the limit of the bipyramidal dimer is facilitated simply by a contact along a common edge or vertex.

The $\mathcal{S}_0$-structure appears to be the optimal packing structure from $\gamma = 1$ to $\gamma \approx 1.63$. On the other end of the asphericity scale, the $\mathcal{D}_0$-structure appears to be optimal from $\gamma \approx 2.19$ to $\gamma = 3$. However, in the intermediate range it appears that both of these structures are suboptimal and different structures take over. For $\gamma \lesssim 1.63$, the density of the $\mathcal{S}_0$-structure increases monotonically with asphericity. However, for the puff with $\gamma \approx 1.63$, contacts between next-nearest layers of the $\mathcal{S}_0$-structure appear, and start to constrain the layer spacing. Assuming no change to the orientations of the puffs and to the construction of the layers, this constraint leads to a sharp drop in the density of the $\mathcal{S}_0$-structure. However, the structure found by the numerical searches shows a

re-orientation of the puffs so that each layer is now composed of puffs of two different orientations (Figure 2). This structure, dubbed the $\mathcal{D}_1$-structure, still leads to a decline in the packing density, but a less dramatic one. Therefore, we have a local maximum in the packing density at the transition from the $\mathcal{S}_0$-structure to the $\mathcal{D}_1$-structure. This transition seems to arise by a continuous deformation of the $\mathcal{S}_0$-structure and is not abrupt. The re-orientation of the puffs suggests the beginning of a tendency towards the dimerization seen in the $\mathcal{D}_0$-structure. However, an intermediate structure is encountered between the $\mathcal{D}_1$-structure and the $\mathcal{D}_0$-structure, producing another local maximum in the optimal density. This structure, to be called the $\mathcal{S}_1$-structure, is a simple (non-dimer) double lattice without the tetragonal symmetries of the $\mathcal{S}_0$-structure (Figure 2), and is reminiscent of the simple double lattice structure reported in Ref. [7]. This structure appears to be separated from the others by an abrupt transition. Figure 3 plots out the densities of the different structures as obtained by the numerical search.

The proper context for the results obtained here for tetrahedral puffs is in comparison to two other one-parameter families of particles that include the sphere as a special case and whose dense packing structures have been investigated vigorously, namely spheroids [1] and superballs [2]. The putative optimal packing of spheroids and superballs becomes monotonically denser the less sphere-like they become. By contrast, the optimal packing density of puffs does not exhibit such monotonicity, although it is always higher than that of the sphere (consistently with a conjecture by Ulam that the sphere is the
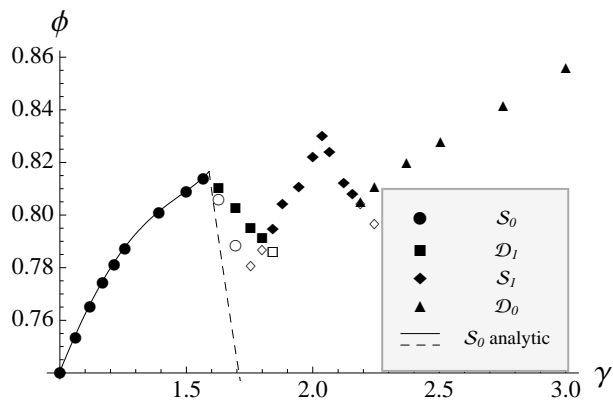
FIG. 3: Highest densities ϕ (filled markers) achieved for packings of tetrahedral puffs of varying asphericity γ. Densities are obtained and reproduced to an accuracy of 0.0005, much smaller than the marker size. The empty markers represent the density attained by a structure at an asphericity where it is suboptimal, as determined either by runs where the search got trapped away from the optimal structure or by runs where the number of particles per unit cell was incompatible with the optimal structure. The two abrupt structural transitions can be easily seen here where the density line for the $\mathcal{S}_1$-structure crosses the lines for the other structures at critical asphericities at which the $\mathcal{S}_1$-structure coexists with them. On the other hand, the continuous structural transition between the $\mathcal{S}_0$- and $\mathcal{D}_1$-structures is associated with a broken symmetry instead: the line corresponds to an analytic construction of the $\mathcal{S}_0$-structure, imposing its tetragonal symmetry. At $\gamma \approx 1.63$, next-nearest layers come into contact with each other, leading to a sharp decline in density (dashed line). If we allow the tetragonal symmetry to be broken, but still allow only two particle orientations, the $D - C$ search produces slightly higher packing densities (empty disks). The $\mathcal{D}_1$-structure obtains higher densities by continuously breaking that symmetry as well.

worst-packing three-dimensional convex solid [22]). Unlike superballs, but like spheroids, the optimal packing of puffs is in all cases (besides the sphere) not a lattice packing, and the crystal unit cell includes at least two particles of different orientations. However, like superballs, and unlike spheroids, the optimal packing structure of puffs goes through an abrupt transition, where two dissimilar structures obtain an equal, optimal density.

A major difference of tetrahedral puffs in comparison to spheroids and superballs is the lack of inversion symmetry. However, not only do the putative optimal packings of puffs in all cases have such a symmetry (Figure 2), it is in some cases the only symmetry of the packing besides its lattice translations. Presumably, inversion symmetry plays an important role in forming close-packed structures of particles with tetrahedral symmetry and maybe even of other particles, a result already observed in the plane by Kuperberg and Kuperberg [21].

The tetrahedral puffs exhibit a much richer optimal packing behavior than either spheroids or superballs, and this richness is likely to be mirrored in the behavior of tetrahedral nano-particles. The variety of qualitatively different dense packing structures observed for mathematical tetrahedra is compounded when a physical shape parameter is added. A possible way to experimentally access the parameter investigated here, which describes a swollen tetrahedron, is by using colloidal particles that swell as a function of their temperature [23]. Thus, a variety of structures and structural transitions could be explored. We have attempted here to provide an atlas of the possible crystal structures which might be observed in systems of particles with tetrahedral symmetry. Our candidates for optimal tetrahedral puff packings provide a starting point for the study of the phase behavior of systems of particles with tetrahedral symmetry, both hard and soft, away from the limit of the mathematical tetrahedron. The method presented here, applicable to any hard convex particle, could also be useful in characterizing possible structures of many other particulate systems.

[1] A. Donev et al., Phys. Rev. Lett. **92**, 255506 (2004).
[2] Y. Jiao, F. H. Stillinger, and S. Torquato, Phys. Rev. E **79**, 041309 (2009).
[3] A. Bezdek and W. Kuperberg (2010), arXiv:1008.2398.
[4] S. C. Glotzer and M. J. Solomon, Nat. Mater. **6**, 557 (2007).
[5] S. Torquato and Y. Jiao, Nature **460**, 876 (2009).
[6] S. Torquato and Y. Jiao, Phys. Rev. E **80**, 041104 (2009).
[7] Y. Kallus, V. Elser, and S. Gravel, Discrete Compu. Geom. **44**, 245 (2010).
[8] M. E. A. Haji-Akbari et al., Nature **462**, 773 (2009).
[9] E. R. Chen, M. Engel, and S. C. Glotzer, Discrete Compu. Geom. **44**, 253 (2010).
[10] A. Jaoshvili et al., Phys. Rev. Lett. **104**, 185501 (2010).
[11] J. Baker and A. Kudrollli, Phys. Rev. E **82**, 061304 (2010).
[12] E. C. Greyson, J. E. Barton, and T. W. Odom, Small **2**, 368 (2006).
[13] Z. Tang et al., Science **314**, 274 (2006).
[14] Z. Quan and J. Fang, Nano Today **5**, 390 (2010).
[15] J. W. Berenschot et al., Nanotechnology **20**, 475302 (2009).
[16] E. Meiner and F. Schilling, Z. Math. Phys. **60**, 92 (1912).
[17] V. Elser, I. Rankenburg, and P. Thibault, Proc. Natl. Acad. Sci. USA **104**, 418 (2007).
[18] Y. Kallus, V. Elser, and S. Gravel, Phys. Rev. E **82**, 056707 (2010).
[19] R. Schneider, *Convex Bodies: The Brunn-Minkowski*

Theory (Cambridge University Press, 1993).

[20] N. J. Higham, in *Applications of Matrix Theory*, edited by M. J. C. Gover and S. Barnett (Oxford University Press, 1989).

[21] G. Kuperberg and W. Kuperberg, Discrete Compu. Geom. **5**, 389 (1990).

[22] M. Gardner, *The Colossal Book of Mathematics* (Norton, New York, 2001).

[23] P. Yunker, Z. Zhang, K. B. Aptowicz, and A. G. Yodh, Phys. Rev. Lett. **103**, 115701 (2009).